

A Data-driven Framework of Resilience Evaluation for Power Systems under Typhoon Disasters

Zhen Yu¹, Mingce Wang², Yinguo Yang¹, Shuangxi Wu¹, Qiuyu Lu¹, Yu Zhu¹, Yang Liu¹, Wei Wang^{2*}, Chao Fang²

¹Electric Power Dispatching Control Center of Guangdong Power Grid Co., Ltd., Guangzhou, Guangdong, China

²School of Management, Xi'an Jiaotong University, Xi'an, Shaanxi, China

(e-mail addresses: shellful@sina.cn (Z. Yu), mingce.wang@stu.xjtu.edu.cn (M. Wang), yangyinguo@gddd.csg.cn (Y. Yang), wusx03@163.com (S. Wu), luqiyu22@126.com (Q. Lu), 47035594@qq.com (Y. Zhu), judy_liuy@126.com (Y. Liu), wwwayne@xjtu.edu.cn (W. Wang, *Corresponding Author), fangchao@xjtu.edu.cn (C. Fang))

Abstract - This paper proposes a data-driven framework of resilience evaluation for power systems under typhoon disasters. A typhoon scenario generation model based on the recurrent neural networks (RNNs) and long-short term memory unit (LSTM) using historical typhoon data are presented. Under generated typhoon scenarios, the resilience of different components of power systems and the entire network are evaluated. We apply the proposed framework to an instance of IEEE-13 bus system to demonstrate its feasibility, and the results prove that our method outperforms in accuracy of resilience assessment than the traditional methods that based on hypothetical typhoon scenarios or single historical typhoon scenarios. Our proposed data-driven framework and the resilience evaluation results can provide system managers with guidance on power system planning and resilience enhancement.

Keywords - Power system, typhoon scenario generation, resilience assessment, recurrent neural networks, LSTM method

I. INTRODUCTION

With the frequent occurrence of typhoon disasters, it poses a huge threat to the operation of power systems and brings vast economic losses. Due to the fragility of critical components (e.g. transmission lines and towers) and the complex network topology between components, the power system disruption event caused by typhoons emerge one after another, resulting in large-scale power outages, which seriously affected economic development and people's livelihood [1, 2]. For example, in July 2014, super typhoon "Rammasun" caused more than 18,000 transmission towers collapsed, about 1,986 kilometers of transmission lines were damaged, and about 2.156 million users were affected in Guangdong Province, China. In July 2021, the severe typhoon "In-Fa" caused a total of 334 transmission line were disrupted and more than 350,000 users' outage in Shaoxing City, Zhejiang Province, China.

To cope with the power system interruption events under extreme weather disasters, the resilience assessment of power systems during their planning process has attracted great attention [3-5]. For instance, Panteli et al. [6]

This work was partially supported by the Science and Technology Project of China Southern Power Grid Corporation under Grant 036000KK52200061 (GDKJXM20202017) and the Natural Science Basic Research Program of Shaanxi under Grant 2021JM-026.

proposed a quantification model of power systems resilience under the real-time impact of severe weather, and randomly generated typhoon scenarios from the assumed probability density distribution of regional wind profiles to test the resilience of the reduced 29-bus Great Britain transmission network. Wang et al. [7] provided a resilience assessment approach for distribution grids under typhoons, and verified the superiority of their method in the IEEE 33 node test system, in which the typhoon parameters (pressure, wind speed, etc.) were determined from the assumed probability density distribution. Ti et al. [8] measured resilience of cyber-physical power systems, and test the performance of the IEEERTS-79 system in the simulated typhoon scenario (the wind speed at each node is derived from a preset probability density function). Liu et al. [9] applied their proposed planning-oriented resilience evaluation method to the IEEE RTS-79 system under the Typhoon Mangkhut scenario, and the resilience ranking of each component is obtained. However, most existing studies measured the resilience of power systems based on hypothetical typhoon scenarios and single historical typhoon scenarios. Considering the high spatiotemporal uncertainty of typhoons, the results of the power system resilience based on traditional methods under different typhoon scenarios still remain to be verified.

In order to provide more reliable resilience evaluation information for decision-making, an emerging trend is to generate a large number of reasonable typhoon scenarios by using learning methods on the historical data. This idea has already been applied to the other fields [10]. For example, Wu et al. [11] used neural networks to generate traffic flow scenarios which can help designing and planning road traffic system. Chen et al. [12] proposed a model-free scenario generation method to simulate the daily production of renewable energy. Hence, to get more reliable power system resilience results, this paper studies a data-driven resilience evaluation method for power systems under typhoon disasters. The main contributions of this paper are three folds.

1) We propose a data-driven framework of resilience evaluation for power systems under typhoon disasters, where a spatiotemporal fragility model and two resilience evaluation indicators for the entire power system and components are involved.

2) A typhoon scenario generation model based on the recurrent neural networks (RNNs) and long-short term memory unit (LSTM) which capture dynamic development

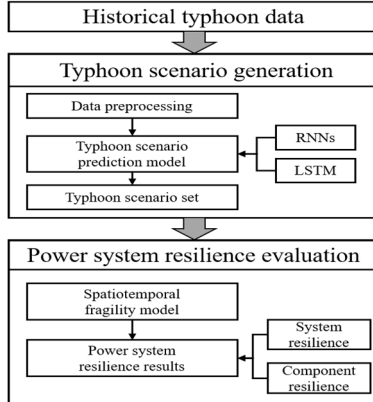


Fig. 1. The data-driven framework of resilience evaluation for power systems

of typhoons is proposed. By using a large amount of historical typhoon data, a lot of reasonable typhoon scenarios are generated, and the resilience of each component of power systems and the entire network are evaluated under typhoon scenarios.

3) We apply the proposed framework to an instance of IEEE-13 bus system to demonstrate its feasibility, and the results prove that the proposed framework in this paper outperforms in accuracy of resilience assessment.

II. THE DATA-DRIVEN FRAMEWORK OF RESILIENCE EVALUATION FOR POWER SYSTEMS

The data-driven framework of resilience evaluation for power systems proposed in this paper is shown in Fig. 1. First, historical typhoon data in the target area is collected. To better fit the typhoon scenario generation model, the data should be preprocessed. Then, the typhoon scenario generation model is proposed to obtain a typhoon scenario set by combining the RNN and LSTM methods. Under the typhoon scenario, the failure probability of each component in power systems is determined based on the spatiotemporal vulnerability model, and finally the resilience of the entire power system and each component can be evaluated. The details of the typhoon scenario generation model, spatiotemporal vulnerability model and the power system resilience evaluation model are described in the following subsections.

A. Typhoon Scenario Generation Model

Due to the complexity and nonlinearity of the atmospheric system, most of the existing typhoon scenario generation methods based on statistical methods have limitations in applications [13]. In this paper, we use RNN to generate typhoon scenarios. RNNs can learn the dynamic time behaviors of complex systems, and simulate the complex nonlinear time relationship of typhoons, and improve the accuracy of typhoon trajectory prediction [14].

Fig. 2 shows a simple schematic diagram of RNN architecture with a depth of 2. The inputs and outputs of the RNN are formatted as time series, which is denoted as

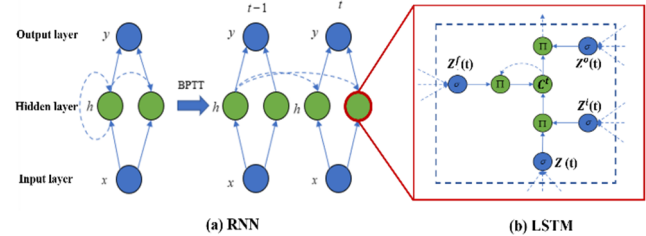


Fig. 2. A simple schematic diagram of RNN architecture used in this paper with a depth of 2

$\mathbf{x} = [x^1, \dots, x^t, \dots, x^T]$ and $\mathbf{y} = [y^1, \dots, y^t, \dots, y^T]$, respectively, where t is the index of the time step. RNN uses backpropagation through time (BPTT) to train neural networks. The hidden neurons h^t in time step t can obtain the input information x^t of the current time step, and the hidden layer information h^{t-1} of the previous time step.

We use the long-short term memory unit (LSTM) to replace the original hidden layer, so as to store information for arbitrary lengths of time steps by preventing the vanish and explosion of weights in the RNN. Since typhoons can last for hundreds of hours, it allows the data from a long time ago of a typhoon to contribute to the forecast of its future track. The illustration of LSTM is shown in Fig. 2(b), where C^t is a memory cell. LSTM selectively stores and utilizes information through input gate Z^i , output gate Z^o and forget gate Z^f . After obtain $Z(t)$, which includes the information of x^t and the h^{t-1} , the LSTM transfers the information to C^t through the $Z^i(t)$, then the $Z^f(t)$ decides whether to store the information, and finally the information is passed to the output layer through $Z^o(t)$. According to this, the output layer can yield y . Thus, we have the typhoon scenario generation model as follows,

$$Z(t) = \tanh(W_{hx}x^t + W_{hh}h^{t-1} + b_h), \quad (1)$$

$$Z^i(t) = \sigma(W_{ix}x^t + W_{ih}h^{t-1} + b_i), \quad (2)$$

$$Z^f(t) = \sigma(W_{fx}x^t + W_{fh}h^{t-1} + b_f), \quad (3)$$

$$Z^o(t) = \sigma(W_{ox}x^t + W_{oh}h^{t-1} + b_o), \quad (4)$$

$$C^t = Z(t) \cdot Z^i(t) + C^{t-1}Z^f(t), \quad (5)$$

$$h^t = \tanh(C^t) \cdot Z^o(t), \quad (6)$$

$$y^t = \text{softmax}(W_{hy}h^t), \quad (7)$$

where \tanh is hyperbolic tangent function, σ is sigmoid function, W represents weights, i.e., W_{hx} is weights between the input layer and the hidden layer, and b_h is a threshold.

After training the model, we use the mean square error (MSE) to evaluate the effect of the obtained model. In the typhoon scenario generation model, the inputs and outputs are sequence data of real and predicted typhoon features (e.g., coordinates, wind speed, wind pressure, etc.), respectively. Therefore, MSE represents the difference between the predicted typhoon features and the real ones.

The predicted typhoon sequence is a new typhoon scenario, and we can generate new scenarios through predictions.

B. Spatiotemporal Fragility Model

A spatiotemporal fragility model is presented to calculate the probability of interruption of a component under a given typhoon scenario. Assuming that the materials, structures, etc. of the transmission lines and towers are homogeneous, the failure probability of component is only related with the wind speed of typhoon at the location of the components[15]. The spatiotemporal fragility model of a component is given as follows,

$$\rho_{jt} = \Phi \left[\ln \left(\frac{V_{jt}}{\mu} \right) / \sigma \right], \quad (8)$$

$$V_{jt} = V_m \left\{ \left(\frac{R_m}{r_{jt}} \right)^\beta \cdot e^{\left[1 - \left(\frac{R_m}{r_{jt}} \right)^\beta \right]^\alpha} \right\}, \quad (9)$$

where ρ_{jt} represents the failure probability of the component j at time t , Φ is the cumulative distribution function of a log-normal distribution, and μ and σ are the mean and variance of the log-normal distribution, respectively. V_{jt} denotes the wind speed of typhoon at the location of the component j at time t , and it is given by Eq.(10). V_{jt} depends on the central wind speed V_m , the maximum wind speed radius R_m and the distance r_{jt} from the location of the component to the typhoon center at that time t . The α and β are constants representing the typhoon profile shape and the proportion of pressure gradient around the radius of maximum wind speed, respectively. In this paper, we set $\alpha = 0.5$ and $\beta = 0.5$.

C. Power System Resilience Evaluation Model

In this subsection, we develop a resilience evaluation model for the power systems and their components. Resilience is measured by the load shedding of the power systems after some components are disrupted under a typhoon scenario. The resilience of the system can be expressed as

$$R_{sys} = \sum_w^W P_w \sum_{t=1}^T \sum_{i=1}^I [(\prod_{j \in \Omega_i} \rho_{jt}) (\prod_{j \notin \Omega_i, j \in J} 1 - \rho_{st})] \Delta I_{wt}, \quad (10)$$

where w is the index of set of typhoon scenarios, and i is index of possible failure scenarios of the power system. I is the number of possible failure scenarios, considering that there are only two states for a component, failed and operational, so when the number of components is n , $I = 2^n$. Ω_i is the set of failed components under failure scenario i . ΔI_{wt} refers to the load shedding of the system under the typhoon scenario w at time t . It is the optimal objective value of network flow model (11)-(16).

$$\min \sum_{i \in N} (\hat{d}_i - d_i), \quad (11)$$

$$\text{s.t } d_i \leq \hat{d}_i, \forall i \in N, \quad (12)$$

$$z_l \cdot \underline{f} \leq f_l \leq z_l \cdot \bar{f}, \forall l \in L, \quad (13)$$

$$d_i = g_i - \sum_{l \in A_i^-} f_l + \sum_{l \in A_i^+} f_l, \forall i \in N, \quad (14)$$



Fig. 3. IEEE 13 bus test system projected to a southeastern coastal area of China

$$g_i, d_i \geq 0, \forall i \in N, \quad (15)$$

$$z_i \in \{0, 1\}, \forall i \in N, \quad (16)$$

where d_i is demand satisfied on node $i \in N$, \hat{d}_i is maximum demand on node $i \in N$. z_l is binary variable which equals to 1 if line $l \in L$ is operational and 0 otherwise. f_l represents Power flow in the line $l \in L$. \underline{f} and \bar{f} are maximum capacity of the transmission line for the forward and reverse transmission, respectively. g_i denotes generated power at node $i \in N$. $A_i^- = \{l \in L: l = (i, j), \forall j \in N\}$ and $A_i^+ = \{l \in L: l = (j, i), \forall j \in N\}$ are set of arcs whose origin and end node are $i \in N$, respectively.

The objective function (11) minimizes the unmet demand, and constraints (12) ensures that the satisfied demand does not exceed the maximum demand, which is reached when the power system have no failed components. Constraints (13) enforce that power cannot be transmitted on damaged lines. Constraints (14) are the flow balance constraint for each node. Constraints (15) and (16) are variable restrictions.

To identify the most vulnerable components, we propose a component resilience assessment model. The resilience of a component is measured by the increment in system resilience by assuming the corresponding component is failed, shown as follow,

$$R_m = R_{sys} |_{P_{wj}=0}, \quad (17)$$

where $R_{sys} |_{P_{wj}=0}$ is the system resilience assuming that the component j will not fail under any typhoon disaster.

III. CASE STUDY

We use IEEE 13 bus test system and project it to a southeastern coastal area of China to demonstrate our resilience evaluation framework for power systems, as shown in Fig.3. The power system has a total of 13 nodes and 14 transmission lines. The total load capacity of the

power system is 1915MW, and the maximum transmission capacity of each transmission line is 5000MW. Demands for each node are indicated in the red circles.

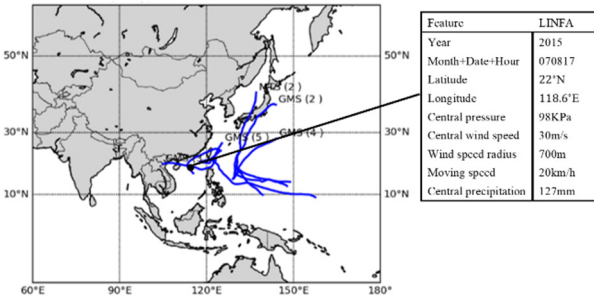


Fig. 4. Top five typhoon trajectories by moving distance and specific data of one typhoon

A. Typhoon Scenario Generation

The dataset used in this paper is original from the *China Meteorological Administration Tropical Cyclone Data Center* (tcdata.typhoon.org.cn), which includes satellite-captured tropical cyclone data from 1980 to 2016 in the southeastern coast, southern coast, and northwestern Pacific Ocean of China. The data set contains a total of 925 complete and different typhoons, and the total data volume is 14998.

To intuitively display the information in the data set, we used the geopy library of Python 3.6 and drawing tools to draw the top five typhoon trajectories by moving distance, as shown in Fig. 4. The figure also shows the specific data of one typhoon at a certain time point.

We process the raw data as follows. According to the latitude and longitude information of the current typhoon time point and that of the initial typhoon time point, we calculate the current moving distance of the typhoon, the offset angle and a location ID that covers the coordinate information.

The RNN-based typhoon scenario generation method in this paper has 8 neurons in the input layer, 12 long-term-short-term memory cells in the hidden layer, and 1 neuron in the output layer. The inputs of the model are latitude, longitude, location ID, central pressure, central wind speed, wind speed radius, moving speed, central precipitation, moving distance and offset angle of typhoon at each time point, and the outputs are latitude, longitude, location ID, central pressure, central wind speed, wind speed radius and moving speed. Before training, we normalize all inputs to numbers between 0 and 1. The 65% (601 typhoons) of the original data set is taken as the training set N^{TR} and 15% (139 typhoons) is used as the test set N^{TE} . The remaining 20% (185 typhoons) is used as an out-of-sample dataset N^{OS} for further analysis later. The number of epochs (time steps) is set to 200, and the batch size is 512. Overall, the training time of the model is fast, about 3 seconds per iteration.

The MSE of the model on the test set N^{TR} is 0.0189, which is very close to 0, indicating that the error between the predicted (generated) scenario and the real scenario is

very small. Fig. 5 shows the comparison between the generated location ID and the real location ID. It shows the linear fit of the first 1000 generated data and the real data,

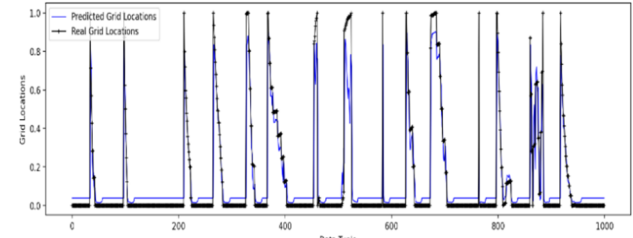


Fig. 5. Comparison between location ID data generated and real data

TABLE I
THE RESILIENCE OF COMPONENTS IN IEEE 13 BUS SYSTEM

| Components (lines) | Resilience | Rank |
|--------------------|------------|------|
| l_1 | 0.874 | 13 |
| l_2 | 0.693 | 12 |
| l_3 | 0.541 | 9 |
| l_4 | 0.255 | 1 |
| l_5 | 0.407 | 6 |
| l_6 | 0.922 | 14 |
| l_7 | 0.497 | 8 |
| l_8 | 0.322 | 3 |
| l_9 | 0.682 | 11 |
| l_{10} | 0.335 | 5 |
| l_{11} | 0.329 | 4 |
| l_{12} | 0.284 | 2 |
| l_{13} | 0.423 | 7 |
| l_{14} | 0.573 | 10 |

and the data is the aggregation of multiple typhoon track information. It can be seen intuitively from the figure that the generated data and the original data are basically fitted.

We finally generated 100 typhoon scenarios and merged them with the typhoon historical scenario set into a typhoon scenario set for subsequent grid resilience assessment.

B. Power System Resilience Evaluation

The power system resilience evaluation model is used to assess the resilience of the IEEE 13 bus system. The system resilience of the power system is 2.742. For each component, the resilience results are shown in TABLE I.

C. Result Analysis

We propose a metric (Eq. (18)) to evaluate the performance of resilience evaluation framework. The differences between the resilience of the power system components under all typhoon scenarios in the out-of-sample dataset N^{OS} and the resilience of the components assessed by our method represent the performance of our proposed data driven resilience evaluation framework. We compare it with the performance of the traditional method. The traditional method we adopted is from [9], which

calculate the resilience of the power system under a single typhoon scenario (i.e., Typhoon “Mangkhut” in 2018). The

TABLE II
THE UNMET DEMAND OF POWER SYSTEM AFTER HARDENING

| | | Our method (MW) | Traditional method (MW) |
|-------|--------------|--------------------|----------------------------|
| $k=2$ | $\eta = 50$ | 787 | 1228 |
| | $\eta = 100$ | 653 | 1011 |
| $k=3$ | $\eta = 50$ | 541 | 963 |
| | $\eta = 100$ | 512 | 885 |
| $k=4$ | $\eta = 50$ | 497 | 829 |
| | $\eta = 100$ | 461 | 783 |

metric of our data-driven power system resilience evaluation framework is 0.031, and the metric of the traditional method is 0.088. Thus, the power system resilience evaluation framework proposed in this paper is more effective than the traditional method.

$$e = \frac{1}{13} \sum_{n=1}^{13} [(R_n - R_n^1) + (R_n - R_n^2)], \quad (18)$$

In addition, we consider that managers can enhance the resistance of power system components under typhoons by strengthening them. Assuming that managers can reduce the failure probability of the k components with the worst resilience by η %, we then observe the resilience of the entire power system after hardening under the typhoon scenarios in the out-of-sample dataset N^{OS} .

We compare the average unmet demand of the power system which is strengthened in the guidance of the component resilience ranking given by our proposed data-driven grid resilience evaluation framework and that by the traditional method under all typhoon scenarios in N^{OS} . The results are shown in TABLE II.

The unmet demand of power system after hardening guided by our method is lower than traditional method. Thus, the power system reinforcement strategy guided by our method outperforms traditional method.

IV. CONCLUSION

This paper proposes a data-driven framework of resilience evaluation for power systems under typhoon disasters. In the framework, a typhoon scenario generation model based RNNs and LSTM are presented. Under typhoon scenarios, the resilience of different components of power systems and the entire network are evaluated.

An instance of IEEE-13 bus system is applied to demonstrate the feasibility of the proposed framework. We propose a metric to test the performance of power system resilience evaluation methods and prove that our method outperforms traditional methods in accuracy of resilience assessment. The resulting resilience ranking of component can provide managers with guidance on power system planning and resilience enhancement.

REFERENCES

- [1] F. H. Jufri, V. Widiputra, and J. Jung, "State-of-the-art review on power grid resilience to extreme weather events: Definitions, frameworks, quantitative assessment methodologies, and enhancement strategies," *Appl. Energ.*, vol. 239, pp. 1049-1065, 2019.
- [2] H. Hou *et al.*, "Damage prediction of 10 kV power towers in distribution network under typhoon disaster based on data-driven model," *Int. J. Elec. Power*, vol. 142, p. 108307, 2022.
- [3] Y. Fang and G. Sansavini, "Optimizing power system investments and resilience against attacks," *Rel. Eng. Syst. Saf.*, vol. 159, pp. 161-173, 2017.
- [4] M. Kamruzzaman, J. Duan, D. Shi, and M. Benidris, "A deep reinforcement learning-based multi-agent framework to enhance power system resilience using shunt resources," *IEEE Trans. Power Syst.*, vol. 36, no. 6, pp. 5525-5536, 2021.
- [5] T. Ding *et al.*, "Power system resilience enhancement in typhoons using a three-stage day-ahead unit commitment," *IEEE Trans. Smart Grid*, vol. 12, no. 3, pp. 2153-2164, 2021.
- [6] M. Panteli, C. Pickering, S. Wilkinson, R. Dawson, and P. Mancarella, "Power system resilience to extreme weather: fragility modeling, probabilistic impact assessment, and adaptation measures," *IEEE Trans. Power Syst.*, vol. 32, no. 5, pp. 3747-3757, 2017.
- [7] Y. Wang *et al.*, "A resilience assessment framework for distribution systems under typhoon disasters," *IEEE Access*, vol. 9, pp. 155224-155233, 2021.
- [8] B. Ti, G. Li, M. Zhou, and J. Wang, "Resilience assessment and improvement for cyber-physical power systems under typhoon disasters," *IEEE Trans. Smart Grid*, vol. 13, no. 1, pp. 783-794, 2022.
- [9] X. Liu *et al.*, "A planning-oriented resilience assessment framework for transmission systems under typhoon disasters," *IEEE Trans. Smart Grid*, vol. 11, no. 6, pp. 5431-5441, 2020.
- [10] R. Yuan, B. Wang, Z. Mao, and J. Watada, "Multi-objective wind power scenario forecasting based on PG-GAN," *Energy*, vol. 226, p. 120379, 2021.
- [11] C. Wu *et al.*, "Spatiotemporal scenario generation of traffic flow based on LSTM-GAN," *IEEE Access*, vol. 8, pp. 186191-186198, 2020.
- [12] Y. Chen, Y. Wang, D. Kirschen, and B. Zhang, "Model-free renewable scenario generation using generative adversarial networks," *IEEE Trans. Power Syst.*, vol. 33, no. 3, pp. 3265-3275, 2018.
- [13] W. Qin, J. Tang, C. Lu, and S. Lao, "A typhoon trajectory prediction model based on multimodal and multitask learning," *Appl. Soft. Comput.*, vol. 122, p. 108804, 2022.
- [14] S. Alemany, J. Beltran, A. Perez, and S. Ganzfried, "Predicting hurricane trajectories using a recurrent neural network," in *Proc. AAAI Conf. on Artif. Intell.*, 2019, vol. 33, no. 01, pp. 468-475.
- [15] D. N. Trakas, M. Panteli, N. D. Hatziargyriou, and P. Mancarella, "Spatial risk analysis of power systems resilience during extreme events," *Risk Anal.*, vol. 39, no. 1, pp. 195-211, 2019.